Optical constants of nickel, iron, and nickel-iron alloys in the vacuum ultraviolet*

T. J. Moravec,† J. C. Rife, and R. N. Dexter
Physics Department, University of Wisconsin, Madison, Wisconsin 53706
(Received 29 October 1975)

Optical constants were obtained by Kramers-Kronig analysis of normal-incidence reflectivities of Ni, Fe, concentrated FeNi alloys, and ordered and disordered Ni_3Fe. Measurements were made from 2 to 27 eV and extended to 35 eV in Ni. Specimens were either thin evaporated films or bulk specimens that were argon-ion sputtered and annealed in ultrahigh vacuum. Data were taken in a mini-computer-controlled vacuum ultraviolet reflectometer at the Wisconsin Synchrotron Radiation Center. The results are described in terms of recent electron energy-band calculations for Ni and Fe and features in the optical conductivity are interpreted in terms of the coherent-potential-approximation theory. Computations of the electron energy-loss function are presented without discussion.

I. INTRODUCTION

The dominant feature of the FeNi system is the ferromagnetism which has led to much study and application.[1] The system has received thorough metallurgical investigation[2] and forms a good example of a disordered binary alloy which has only one ordered phase and is easy to prepare. Random disordering has recently been reviewed by Elliott, Krumhansl, and Leath[3] and, in context, they discuss one very successful approach to the description of a binary alloy, namely, the coherent-potential approximation (CPA). By an extension of the work of Velický, Kirkpatrick, and Ehrenreich,[4] who applied the CPA to simple binary alloys, Hasegawa and Kanamori (HK), in a series of papers,[5] discussed the FeNi system within the CPA framework with considerable success. They showed that both fcc-disordered NiFe and bcc-disordered FeNi were systems for which the approximations of the CPA were particularly sound.[6] A portion of those papers dealt with the expected changes of the electronic band structure as evidenced by the density of states and its components which were owing to the Fe and Ni fractions, separately. We will first consider whether we can expect to see manifestations of these subtle changes of densities of states in the optical properties on alloying Fe and Ni.

Optical studies to delineate the electronic band structure of metals or help to clarify the theory of disordered binary systems must contend with certain negative features. In the case of FeNi these features include the change of crystal structure from bcc to fcc when the Ni content exceeds about 25%, and perhaps other phase changes as well. A far more serious difficulty is that optical features are generally very broad in the $3d$ transition metals and identifiable critical points are not commonly found for the pure elements or ordered alloys. For the disordered alloys the optical features might be expected to be even broader. In addition, with the loss of long-range order, a $\vec{k}$-space description within traditional band theory is no longer applicable. The distortions of band structure expected in the density of states[5] (which remains a useful concept in CPA) might well be submerged within the bland lifetime-broadened optical features, and therefore not easily be subject to confirmation. We shall see that in FeNi the optical conductivity σ of disordered alloys is very similar to that of the pure metals, both being rather broad. Many aspects of the description of the origins of the optical properties will therefore be ambiguous even though those properties appear to be quite definite. Nevertheless, from prior work it is known that a major optical feature in Ni at 4.6 eV probably arises from interband transitions within the minority spin bands ($\downarrow$) and, in fact, from flat regions of high density of states. These regions are precisely those which deform most significantly in the CPA model.[5] We conclude that it is realistic to look for significant changes of optical features for ultraviolet photons upon alloying Fe and Ni.

There have been extensive studies of the optical properties from near 0 to 5 eV in Ni,[7–13] Fe,[14,15] and both[16,17] although the interpretation of these properties is still in question.[18] Gorban *et al.*[19] have measured the optical constants for several concentrations of Ni-rich NiFe from 1.1 eV to 4.9 eV and we will be using their results at low energies. Vehse and Arakawa[20] measured the reflectivity $R(E)$ of Ni up to 25 eV, and Blodgett and Spicer[21] measured $R(E)$ for Fe up to 11 eV. In general our results are in good agreement with previous observations although absolute reflectivities generally disagree by a few percent between all observers. New results presented here include $R(E)$ for Ni from 25 to 35 eV, Fe from 11 to 27 eV, and NiFe from 5 to 27 eV including numerous concentrations for which no previous measurements have been reported such as ordered and disordered Ni_3Fe.

The usual procedure for interpreting the electronic structure of solids[8] is to identify peaks in ϵ_2, the imaginary part of the dielectric constant, or σ, the optical conductivity (which is proportional to $\omega\epsilon_2$), with transitions within energy bands of one-electron band calculations. ϵ_2 is obtained from a Kramers-Kronig (KK) inversion of $R(E)$.[22] This procedure has been moderately successful for other transition metals.[23-26] A good example of more difficult attempts to interpret the optical properties of an alloy is provided by the study of Scott and Muldawer[27] on reflectivity and ϵ_2 in ordered and disordered Cu_3Au where new features arise in the optical spectrum of the ordered phase. Further discussion of optical and photoemission work on metals and alloys will be found in the review of Nilsson.[18] Successes of the CPA formalism in discussing optical properties are further detailed by Nilsson with specific examples such as the CuNi system which has been investigated further by x-ray photoemission spectroscopy[28] and by soft-x-ray spectroscopy.[29] The relevance of the work on CuNi to the present observations is not direct, since for CuNi the split-band instead of single-band regime[4] of CPA is applicable, but lessons there about the application of CPA to real systems should aid us in the present work.

For about half of the present energy range of observations there exist a number of one-electron band calculations for ferromagnetic Ni and Fe. Recent calculations for Ni by Wang and Callaway[30] and for Fe by Singh, Wang, and Callaway[31] appear to be particularly useful for describing many physical properties of these two metals. The interpretation of structure in the real optical conductivity for Ni and Fe will be based on the above calculations. After a brief description of the experimental apparatus and sample preparation, we will present the experimental results and discuss their interpretation.

II. EXPERIMENT

The experimental arrangement is the same as that recently described in work on alkali halides.[32] Briefly, ultraviolet radiation from the electron storage ring at the Physical Sciences Laboratory of the University of Wisconsin is monochromatized and made to impinge on the specimen. This radiation is substantially linearly polarized in the plane of reflection and is incident at an adjustable angle near 11° to the normal. The reflected light is converted to about 400-nm wavelength by sodium salicylate on a rotatable light pipe and pulses are detected by a photomultiplier. Incident light intensity and electron-beam current are also monitored and the results utilized in computation of a reflectivity which is corrected for background, scattered light, dead time in counters, etc. The entire experiment is under control of a PDP $8/E$ minicomputer and details may be found elsewhere.[32-34] A clean environment is provided by the ultrahigh vacuum maintained by ion pumps which also pump the electron storage ring and all other chambers attached to it.

Most of the samples studied were evaporated onto clean slides[34] using NiFe alloy strips which were made by powder-metallurgical techniques in a concentration range near the desired film concentration. It was seldom that the final concentration of the film was close to that of the bulk. The strips were placed in tungsten, stranded baskets or molybdenum strips coated with Al_2O_3 to reduce alloying with the molybdenum. The evaporation techniques used were those described by Holland.[35] Films were evaporated in a chamber pressure of 10^{-8} Torr and quickly vacuum transferred into the experimental chamber which was maintained in the pressure range of about 5×10^{-10} Torr.

The films varied in thickness from 20 to 70 nm and this thickness was measured during deposition with a quartz-crystal thickness monitor. The film concentration was determined after the data were recorded by a scanning electron microscope technique.[36] For the system Ni_xFe_{1-x}, x could be determined to about $\pm$ 0.03 or better. Although the film concentration varied from that of the bulk as expected, enough specimens were evaporated to give a broad range of concentrations. Bulk specimens were used as a check and to fill in gaps in the composition range. During measurements, specimens could be freely interchanged at high vacuum between the reflectometer and preparations chamber.

A possible confusion would have occurred in our measurements if the films had been composed of small islands or clusters[37,38] of Ni or Fe. Then the reflectivity might have been just a weighted average of the two constituents in their normal bulk phases. This clustering was not expected because of the results of previous studies of this alloy system.[39] To within the 20-nm resolution of the scanning electron microscope no islands were found. A more serious artifact might have occurred if the deposition had been in the form of a sandwich layer of the two constituents. Such a sandwich was earlier made in CuNi by Gudat and Kunz[29] to illustrate in an ingenious way the averaging of soft-x-ray absorption spectra. Such a sandwich would not have been detected by the scanning-electron microscope in our measurements. Here the FeNi system provides a natural way to eliminate the suspected presence of the artifacts. Sandwich or clustering inhomogeneities would leave the Fe in the bcc phase for most concentrations. The

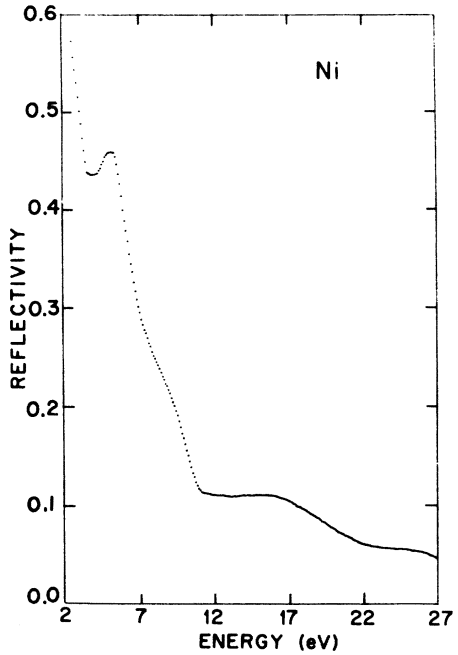

FIG. 1. Measured normal (11°) incidence reflectivity of nickel from 2 to 27 eV at 0.1-eV intervals.

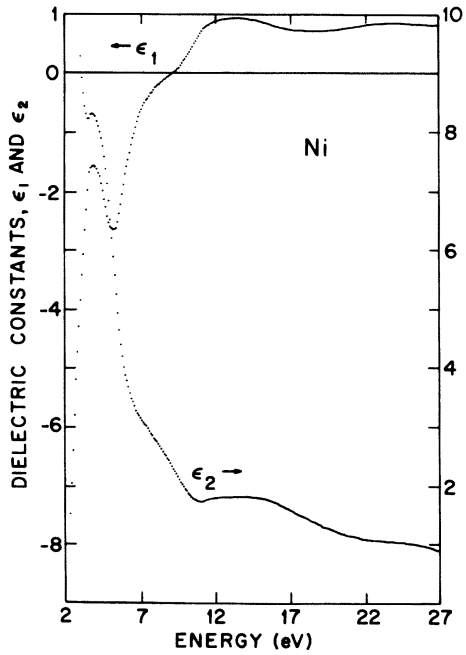

FIG. 3. Real (ϵ_1) and imaginary (ϵ_2) parts of the dielectric constant versus energy for nickel calculated from KK analysis.

averaging of bcc Fe reflectivity with fcc Ni reflectivity does not closely resemble the observed spectrum of an fcc NiFe alloy. We can be confident that at least two artifacts of film preparation are not important in this work.

Three specimens were polished bulk specimens that were annealed in vacuum by radio-frequency induction heating and/or cleaned by argon-ion bombardment from a sputter-ion gun. The polishing was done on a lapping apparatus in the usual manner utilizing progressively finer abrasives. The final polish was made with Syton as described for Ni recently.[13] It was observed that the ion bombardment changed the ordering of the alloy sufficiently far into the surface that the reflectivity spectrum closely resembled that of the evaporated film of a similar concentration. Since this technique, if sound, permitted the production of a disordered state similar to that produced by quenching from high temperature we discuss it further with the results in Sec. III. Whether or not the technique is sound, the major thrust of the measurements was on disordered evaporated specimens and bulk specimens were utilized to reach a specific desired composition. We now describe the results of the measurements.

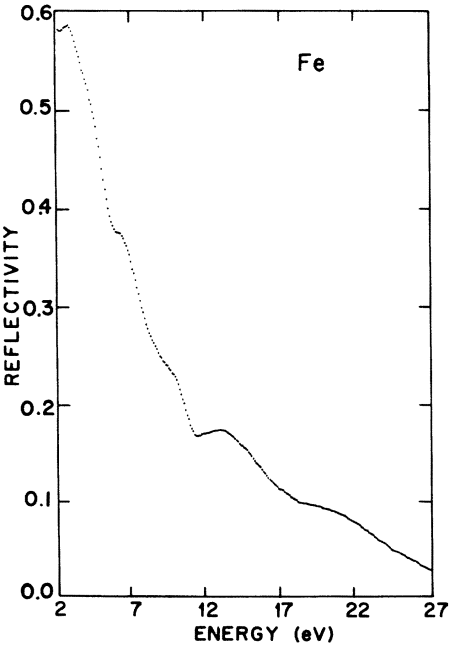

FIG. 2. Measured normal (11°) incidence reflectivity of iron from 2 to 27 eV at 0.1-eV intervals.

III. EXPERIMENTAL RESULTS

All figures of experimental reflectivity in this paper are computer-plotted files with smoothing, derivatives, etc., generated directly from the minicomputer. Figure 1 shows near-normal incidence $R(E)$ for Ni, and Fig. 2 shows $R(E)$ for Fe from 2 to 27 eV. The corresponding calculated ϵ_1 and ϵ_2 curves are shown in Figs. 3 and 4, respectively. Although data were taken at 0.02- or 0.05-eV intervals, optical constants were evaluated

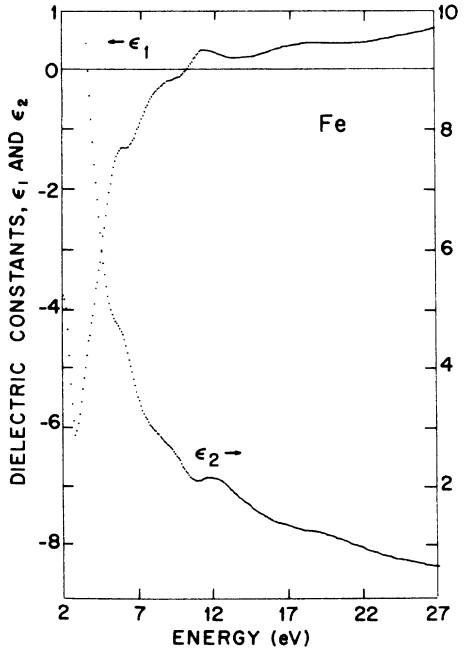

FIG. 4. Real (ϵ_1) and imaginary (ϵ_2) parts of the dielectric constant vs energy for iron calculated from KK analysis.

only at 0.1-eV intervals since no resolution was apparently lost.

For the Ni and Fe optical constants below 3 eV we used a best fit among the earlier works and extrapolated our data from about 3 eV down to 0.5 eV for both Ni and Fe. For the alloys that were measured by Gorban *et al.*[19] our data were fit to theirs in the extrapolation region. For the other FeNi alloys, the reflectivity was interpolated between values for Fe and Ni and then extrapolated from 3 to 0.5 eV. Clearly, no trust may be put in conclusions derived from this method in the energy range below 3 eV. However, this method was utilized so that the low-energy function used in the KK program to extrapolate to zero was matched at 0.5 eV instead of at 3 eV. The parameters for the 0.5 eV function were chosen by the method of Veal and Paulikas.[40]

For the high-energy end also, the procedures used by Veal and Paulikas were followed. The parameters for the one Drude oscillator function were chosen so as to match the magnitude of the reflectivity at 27 eV and following inversion to scale the derived ϵ to a reasonable fit. For extrapolations we used a compromise in the 2–5-eV range of the data of Gorban *et al.*,[19] Johnson and Christy,[17] and Yolken and Kruger.[14] The high-energy oscillator fit did not affect structure in the measured range, only magnitude as previously noted.[22,40] In addition, the $n-1$ and n_{eff} sum rules[41] were monitored to keep the extrapolation physically plausible. The estimated absolute accuracy of the KK-generated n and k values is (10–15%) based on the extrapolation uncertainty and the (2–3%) absolute error in the reflectivity. Relative errors are much smaller.

Figure 5 shows $R(E)$ between 9 and 18 eV at higher resolution to point out the constancy of the edge at 10.5 eV which occurs throughout the alloy series independent of crystal structure or order. The data for the $Fe_{0.62}Ni_{0.38}$ alloy are characteristic in this range of all the fcc disordered alloys.

Figure 6 is a composite showing the reflectivity at room temperature of Ni, Fe, and several alloys in between. Data below 3 eV were considered unreliable due to nonuniformities in the sodium salicylate coating which partially transmits radiation and does not fluoresce at this low-energy range. The $R(E)$ of Ni was measured out to 35 eV (not shown) and was found to be featureless with a gentle-slope downward. Data for Ni, Fe, and some alloys were also taken at 100 K but no striking changes in magnitude or sharpness of structure were noted between the data at the two temperatures and we only describe results from 300 K observations. Our $R(E)$ values agree well with other studies at lower energies.[8,10,19–21] The high-energy end for these metals is very characteristic of other transition metals.[23–26]

Curve i in Fig. 6 is a bulk $Ni_{0.74}Fe_{0.26}$ alloy that was annealed for 30 min in ultrahigh vacuum. More broad structure can be seen between 10 and

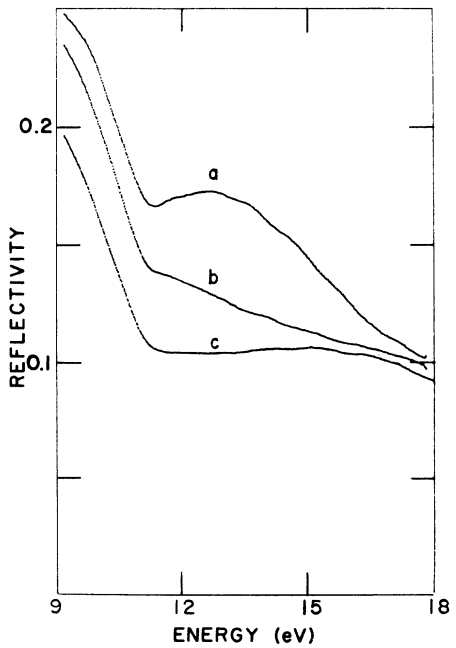

FIG. 5. Reflectivity near the assumed free-electron plasma edge at 0.02-eV intervals. Curves (a) Fe, (b) $Fe_{0.62}Ni_{0.38}$, and (c) Ni.

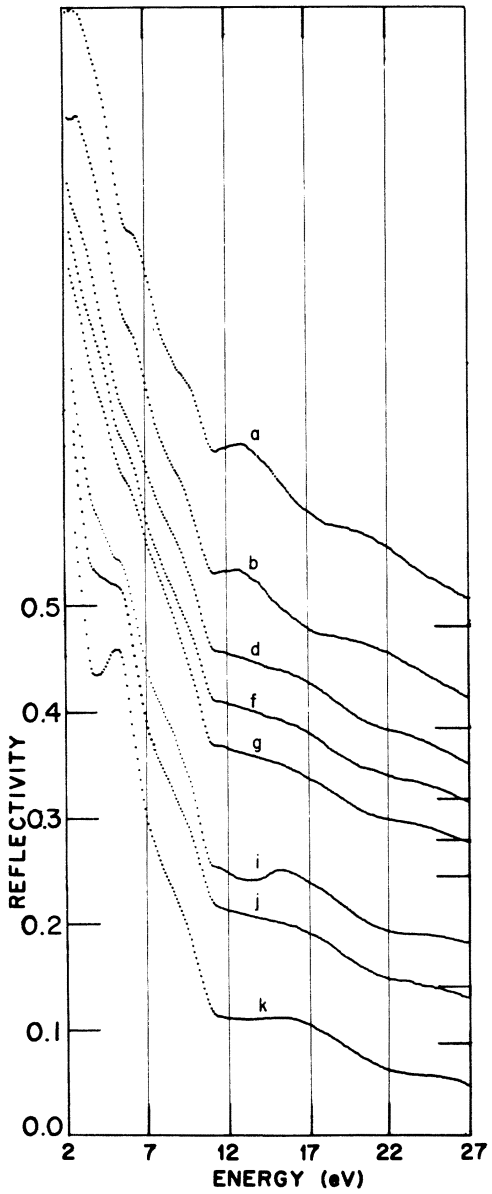

FIG. 6. Composite of some of the reflectivities studied. The scale is shown for the bottom curve. The zeros of the others are offset in relation to their concentration and are shown at the right. The letters designate the following Ni concentrations: (a) 0.0, (b) 0.20, (c) 0.24, (d), 0.34, (e) 0.38, (f) 0.42, (g) 0.49 (bulk, sputtered only), (h) 0.69, (i) 0.74 (annealed only), (j) 0.77, and (k) 1.00.

17 eV than occurs in Ni or Fe, and the 20-eV peak changed shape and magnitude. Other regions of the spectrum for $Ni_{0.74}$ showed little change from other nickel-rich alloys. This specimen was run through the sequence of steps shown in Fig. 7. Curve (a) is the reflectivity of the sample after it was etched in air[21] and placed into a chamber which was immediately pumped out. The difference from the vacuum-handled specimens indicates the probable flaws which would be found in results from air-etched specimens in the vacuum ultraviolet for FeNi alloys. Curve (b) in Fig. 7 was observed after 30-min ultrahigh vacuum anneal at about 1000 K. The amount of structure is indicative of considerable long-range order. Curve (c) in Fig. 7 was taken after a 1 min argon-ion sputter. The rather featureless curve is very similar to that found for evaporated films of similar composition. For this reason we believe the sputtering destroyed the long-range order to the depth that the photon beam can sample and, in effect, made it disordered like the thin films. The specimen was then annealed for 30 min and curve (d) was observed. The similarity to curve (b) suggests that long-range order has been partially restored despite the short annealing times. All of the above steps were taken without exposing the specimen to air. The slight lowering in magnitude for curve (d) is probably not significant since independent runs on the same surface often led to reflectivity variations within a 3% absolute reflectivity range.

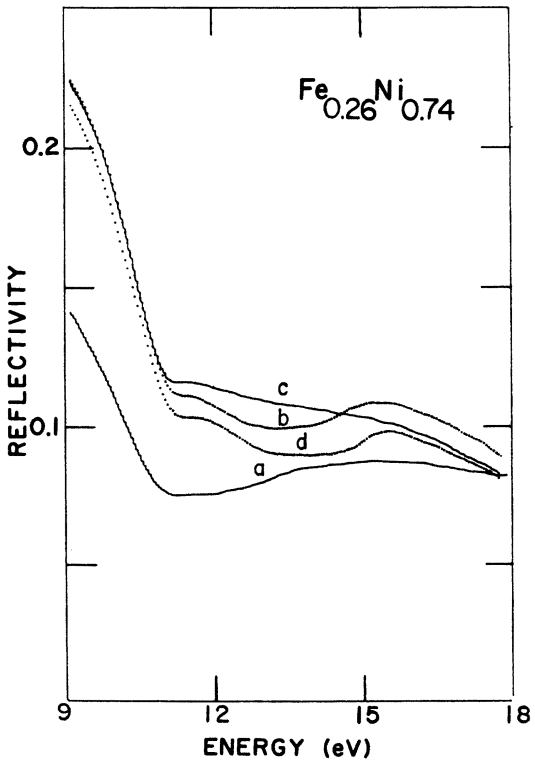

FIG. 7. Energy region of most difference in reflectivity between ordered and disordered $Fe_{0.26}Ni_{0.74}$ bulk alloy. The data were taken in the following sequence: Curve (a) etched sample, (b) after $\frac{1}{2}$-h anneal at about 1000 K, (c) after 1-min sputter, and (d) after additional $\frac{1}{2}$-h anneal.

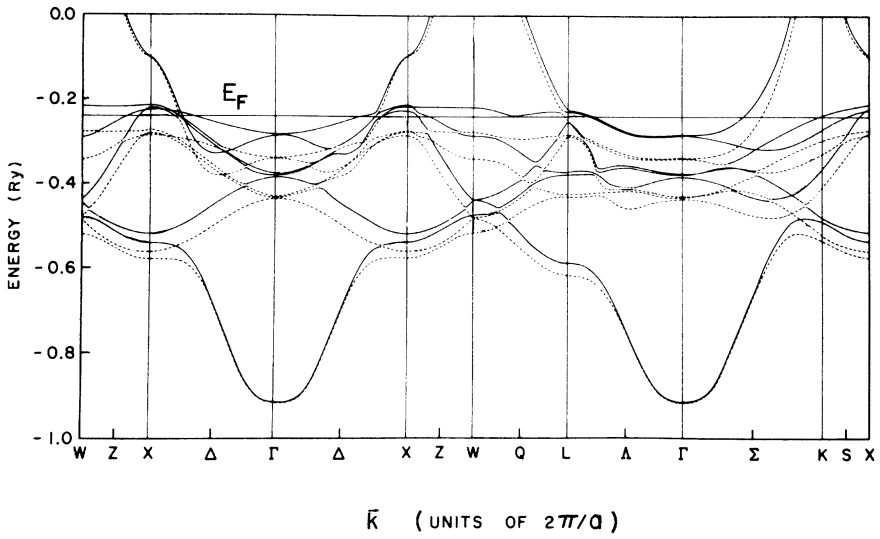

FIG. 8. Band structure of nickel along some symmetry lines in the BZ. States are labeled according to symmetry of the largest spin component. The solid lines indicate states of minority spin; the dashed lines indicate those of majority spin. From Wang and Callaway (Ref. 30).

This method of disordering the surface was used with several bulk specimens which had mixed-phase character prior to the sputtering. It permitted us to reach alloy ranges which were not included in the accidental concentrations obtained by evaporations and without quenching bulk specimens from high temperature. X-ray tests for ordering have not yet been performed.

IV. DISCUSSION

According to traditional band theory peaks in σ correspond closely to peaks in the joint density of states (JDOS) and are identified with direct transitions in the band structure. Figure 8 shows the bands for Ni as calculated by Wang and Callaway[30] and Fig. 9 shows those for Fe as calculated by Singh, Wang, and Callaway.[31] The 4.6-eV peak in σ in Ni is often associated with transitions around the L point[8,9,19] and the 2.5-eV peak in σ for Fe with transitions in the zone face (direction F and points P in Fig. 9).[31] It is unclear why the optical data for the alloys so closely resemble that of the pure elements since the Brillouin-zone (BZ) description is not applicable to the alloys. In Fig. 10 new peaks are seen in σ(Fe) at 6.1, 9.4, 12.6, and 19.1 eV. The 6.1-eV peak appears to move to lower energy, persists in the alloys through the change in crystal structure, and still remains in the Ni-rich alloys. It seems to become a part of the 4.6-eV peak in Ni. A large portion of the BZ must be involved in the 4.6-eV peak owing to its size. Moreover, the Ni band structure shows

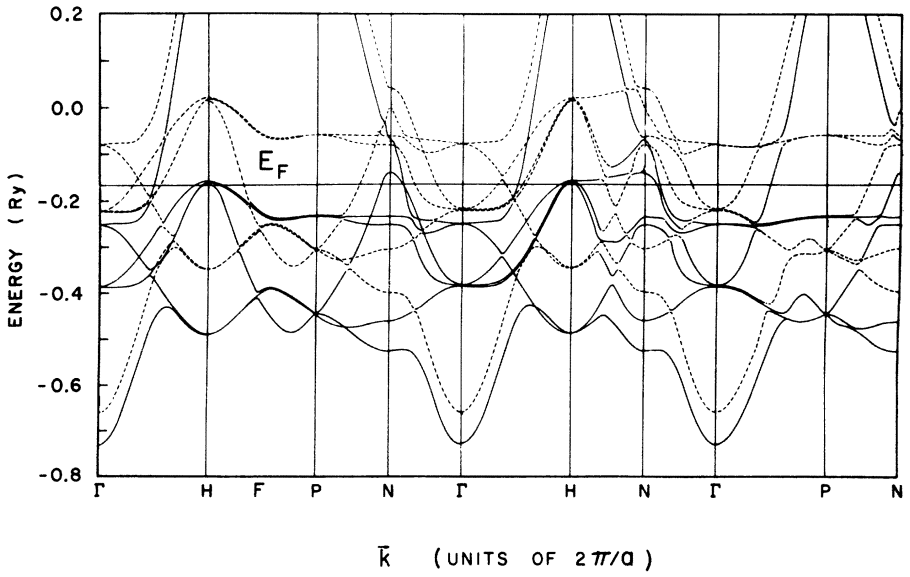

FIG. 9. Band structure of iron along some symmetry lines in the BZ. The spin-alignment direction is [011]. States are labeled according to the symmetry of the larger spin component. The solid lines indicate states of majority spin; the dashed lines indicate those of minority spin. From Singh, Wang, and Callaway (Ref. 31).

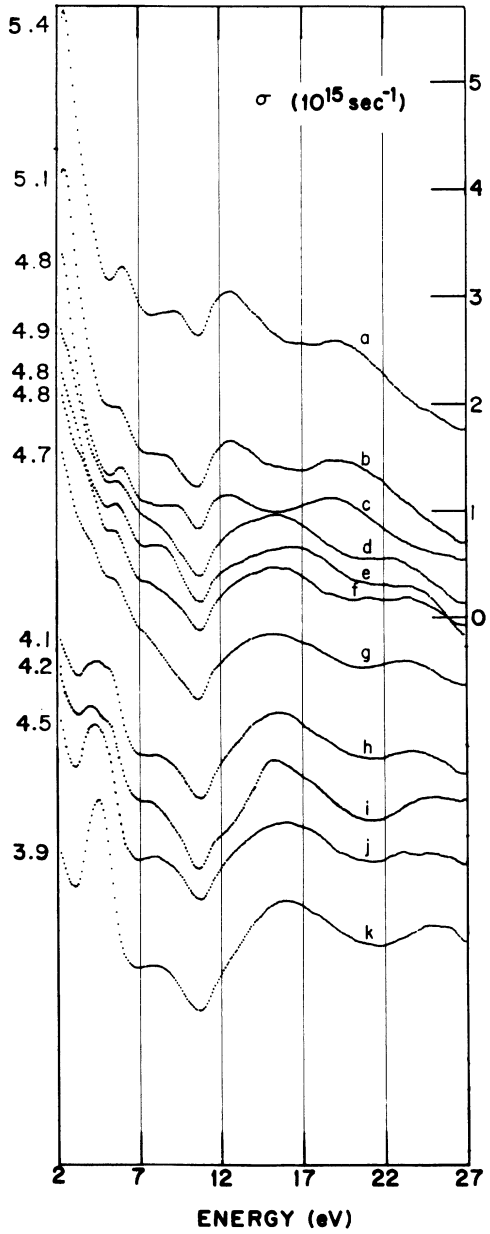

FIG. 10. Composite of some of the computed optical conductivities. The scale is shown for curve (a) while others have their zeros offset down in proportion to their concentration. The value that σ obtained at 2 eV is shown on the left for each curve. Letters designate the same Ni concentrations as described in the caption for Fig. 6.

many flat and parallel regions with roughly this energy separation.[8,30] The large area involved makes it appropriate to describe the optical properties of the pure elements in the density-of-states language which is the natural language used for describing alloys.

It is somewhat surprising that the structure in σ near 5 eV remains through the fcc-bcc phase transition, whereas there is a large change in shape at the high-energy end. This abrupt change takes place near the expected concentration[2] range of $Fe_{0.7}Ni_{0.3}$. Other similarities in structure are evident when Fe and Ni are compared. Ni has a peak at 8.0 eV similar in shape to the 9.4-eV peak in Fe. The two broad peaks in Ni near 16 and 25.5 eV may be compared to the slightly sharper ones at 12.6 and 19.1 eV in Fe. Despite the difference in crystal structure the curves are qualitatively similar. Upon adding Fe to Ni the total number of electrons decreases but according to the simple CPA model of HK the number of majority spin electrons ($\uparrow$) remains constant up to about $Fe_{0.5}Ni_{0.5}$ and the density of states of the ($\uparrow$) band keeps its original shape. The calculations indicate that the deformation of the minority spin bands ($\downarrow$) for both the Fe and Ni fractions is largest in the energy ranges corresponding to the final states of transitions assumed to account for the 4.6 eV peak in Ni.

Onodera and Toyozawa[42] investigated the theory of the optical spectra of substitutional binary alloys in the CPA formalism and applied the results to observations on mixed alkali halides. They and also Velický, Kirkpatrick, and Ehrenreich[4] noted that the most important parameter that determined the character of change of density of states was the ratio of the difference of the energies of the two individual components to the width of the energy band itself. When this ratio is small, as is the case for FeNi, the individual bands although deformed unite to give a single band, and the optical structures are amalgamated. Familiar examples of this optical behavior are found in many semiconductor systems, such as GaP-GaAs,[43] and in the extreme limit the virtual crystal approximation is recovered from the CPA description.

The deformation of the density of states of FeNi is compatible with a splitting of transitions for which the final state is just above the Fermi energy.[5] Unlike the case for NiCu where the density of states has been shown[28,29] to fulfill the prediction of the split-band regime, the results of our study are much closer to the virtual crystal regime. Consider Fig. 10. Apparently the 4.6-eV peak in Ni splits into two peaks. In Fig. 8 we observe that large portions of the BZ are separated from empty states by about the same energy which could easily be 4.6 eV. These portions include regions near X, L, and Σ. Shifts in the JDOS are expected on alloying. We speculate, by noting separations of energy in Fig. 9 for bcc Fe (a different BZ), that shifts in JDOS which peaked near X in Ni, might move to lower energy becoming peaks near P and F in Fe at 2.5 eV. Transitions near L and Σ in Ni also lead to high JDOS near 4.6 eV

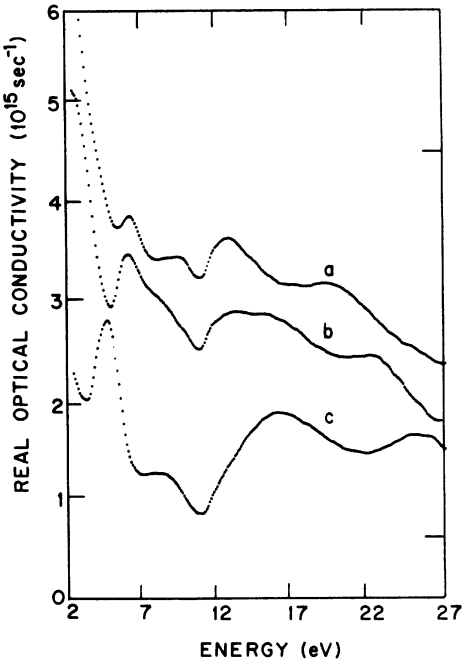

FIG. 11. Optical conductivities for (a) bcc Fe, (b) synthetic conductivity for fcc iron computed from data for the $Ni_{0.34}$ specimen and pure Ni, (c) Ni. The scale is shown for curve (b), while the maximum value and zero of the scale are shown on the right for curves (c) and (a).

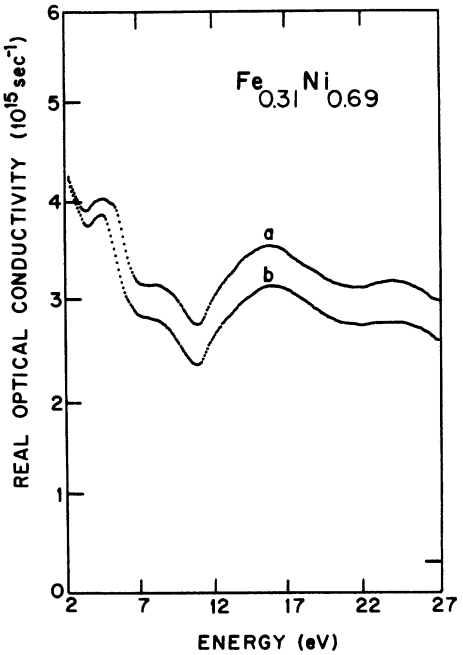

FIG. 12. Optical conductivities for the alloy $Fe_{0.31}Ni_{0.69}$ (a) computed by KK analysis from measured reflectivity. (b) calculated from synthetic-fcc iron conductivity and conductivity of nickel as explained in the text. The scale is shown for curve (b). The zero is shown at the right for curve (a).

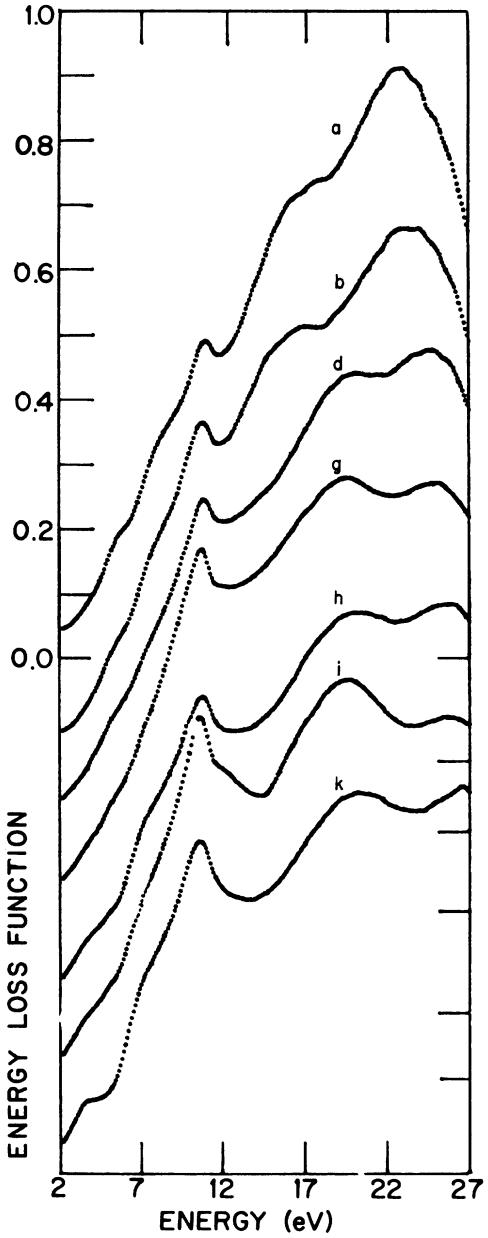

FIG. 13. Composite of some of the computed $\mathrm{Im}(-1/\epsilon)$ curves. The scale is shown for curve (a) while others have their zeros offset down in proportion to their concentrations as shown on the right-hand side. The letters designate the same specimens as in Fig. 6.

which might move to higher-energy extrapolating to a peak in Fe at 6.1 eV perhaps along Σ for which the energy spacing of Fig. 9 provides a suggestive separation. The 2.5-eV peak in Fe might be observed to split or have an important component which moved to lower energy in Ni.[44] That component in Ni would correspond to transitions between the nearly parallel upper *d* bands of opposite spins near the zone face which are allowed with

small matrix elements, and which then would be a measure of the exchange splitting responsible for ferromagnetism. There are no optical studies on Fe-rich bcc alloys which might have clarified this point. Our observations are qualitatively similar to those for AuAg but there charge transfer theory is involved.[18,45]

The motion and shapes of the 8- and 16-eV peaks in Ni are difficult to follow through the alloy series, in part because of the dominating effect of the persistent 10.5-eV plasma structure. The broad 25.5-eV peak in Ni shifts rather linearly with concentration of Fe to lower energy until the phase transition. One result of the CPA theory is that if the scattering strengths of the potential are not too strong then one could expect σ for the alloy to be the weighted sum of the conductivities of the two constituents.[3] Those conductivities will to some degree mirror the deformations of the density of states. Little deformation can be assumed for the initial states in the $\uparrow$ or $\downarrow$ bands.[5] To compute a weighted-average conductivity it is first necessary to compute a synthetic conductivity for fcc Fe, $\sigma_{fcc}(\mathrm{Fe})$. We use the weighted average assumption. For a concentration x of Ni,

$$(1-x)\sigma_{fcc}(\mathrm{Fe}) = \sigma(\mathrm{Ni}_x) - x\sigma(\mathrm{Ni})\,. \tag{1}$$

The fcc alloy with the largest Fe content in our work is the $\mathrm{Ni}_{0.34}$ thin film. $\sigma_{fcc}(\mathrm{Fe})$ was computed from Eq. (1) and the result is plotted in Fig. 11 along with $\sigma(\mathrm{Fe})$ and $\sigma(\mathrm{Ni})$ for comparison. It is in accord with the general model of HK that $\sigma_{fcc}(\mathrm{Fe})$ is similar to $\sigma(\mathrm{Ni})$. Since we have assumed no deformation, different alloys might have generated quite different $\sigma_{fcc}(\mathrm{Fe})$ curves. In fact, they are rather similar in character. Conversely, a weighted-average conductivity can be calculated for any fcc alloy from the synthetic $\sigma_{fcc}(\mathrm{Fe})$ and observed $\sigma(\mathrm{Ni})$ again on the assumption of no deformation. This was attempted for a number of alloys by inverting Eq. (1) to solve for $\sigma(\mathrm{Ni}_x)$. An example of such a computation is shown in Fig. 12 for $x=0.69$. The top curve is the actual σ obtained from KK analysis and the bottom curve is calculated from Eq. (1) using data from $x=0.34$ and $x=1$. With some exceptions the calculated curves reproduce well the actual $\sigma(\mathrm{Ni})$ curves for all fcc alloys. Owing to the limited range of Fe-rich bcc alloys, we did not try to compute a synthetic $\sigma_{bcc}(\mathrm{Ni})$.

The motion of the 4.6-eV peak in Ni which we discussed in terms of a deformation origin above is obviously not reproduced by a weighted averaging of the end-point conductivities, nor should it be since this energy range is one where the effects of deformation would be most profound. Another disagreement with the weighted averaging of end points is found for the highest-energy peaks. The actual σ is always sharper than would be expected from averaging although the position in energy agrees well. For a peak to appear at 25 eV in Ni with a width of several eV, the entire s-d band would be involved in the initial state of the transition (which terminates well above the vacuum level). We will not speculate here on the origin of a peaked JDOS so far above the ranges of existing band calculations.

Finally, we present the loss functions derived from our KK analysis. The computed Im $(-1/\epsilon)$, shown in Fig. 13, may be expected to correlate well with the energy loss of transmitted or reflected electrons.[46-48] Electron loss in transition metals is in a theoretical regime difficult to treat and we will not further discuss our results.

ACKNOWLEDGMENTS

We wish to thank E. Rowe, C. H. Pruett, R. Otte and the staff of the University of Wisconsin Physical Science Laboratory Synchrotron Radiation Center for providing the stable and intense vacuum-ultraviolet source. Helpful discussions are acknowledged with J. H. Weaver, C. Olson, C. C. Lin, and S. P. Bowen. K. K. Rao and S. Prawirosusanto were of great assistance in development of the computer aspects of this research and bulk specimen preparations, respectively. We also thank B. W. Veal for providing us a copy of his KK analysis program and Everett Glover for his assistance with the scanning electron microscope. We also acknowledge an informative letter from C. P. Wang concerning the band structures of Fe and Ni. During the period of this research, the storage ring was operated with funds from AFOSR and later by NSF under operations Grant Nos. AFOSR-F44620-7-0-0029 and DMR-74-15089, respectively.

*Supported in part by the Air Force Office of Scientific Research under Grant No. AFOSR-70-1906 and in part by The Wisconsin Alumni Research Foundation.

†Present address: Physics Dept., Rice University, Houston, Tex. 77001.

[1]R. M. Bozorth, *Ferromagnetism* (Van Nostrand, New York, 1951).

[2]M. Hansen, *Constitution of Binary Alloys* (McGraw-Hill, New York, 1958).

[3]R. J. Elliott, J. A. Krumhansl, and P. L. Leath, Rev. Mod. Phys. 46, 465 (1974).

[4]B. Velicky, S. Kirkpatrick, and H. Ehrenreich, Phys. Rev. 175, 747 (1968).

[5]H. Hasegawa and J. Kanamori, J. Phys. Soc. Jpn. 31, 382 (1971); H. Hasegawa and J. Kanamori, J. Phys. Soc. Jpn. 33, 1599 (1972).

[6]J. Kanamori, J. Appl. Phys. 36, 929 (1965).

[7]S. Roberts, Phys. Rev. 114, 104 (1959).

[8]H. Ehrenreich, H. R. Philipp, and D. J. Olechna, Phys. Rev. 131, 2469 (1963).

[9]M. Shiga and G. P. Pells, J. Phys. C 2, 1847 (1969).
[10]J. Feinleib, W. J. Scouler, and J. Hanus, J. Appl. Phys. 40, 1400 (1969).
[11]D. W. Lynch, R. Rosei, and J. H. Weaver, Solid State Commun. 9, 2195 (1971).
[12]P. B. Johnson and R. W. Christy, Phys. Rev. B 11, 1315 (1975).
[13]A. A. Stuona, Solid State Commun. 16, 1063 (1975).
[14]H. T. Yolken and J. Kruger, J. Opt. Soc. Am. 55, 842 (1965).
[15]G. A. Bolotin, M. M. Kirillova, and V. M. Mayevskiy, Fiz. Metal. Metalloved. 27, 224 (1969).
[16]M. C. Jones, D. C. Palmer, and C. L. Tien, J. Opt. Soc. Am. 62, 353 (1972).
[17]P. B. Johnson and R. W. Christy, Phys. Rev. B 9, 5056 (1974).
[18]P. O. Nilsson, in *Solid State Physics*, edited by H. Ehrenreich, F. Seitz, and D. Turnbull (Academic, New York, 1974), Vol. 29, p. 139.
[19]N. Ya. Gorban, V. S. Stashchuk, A. V. Shirin, and A. A. Shishlouskii, Opt. Spectrosc. 35, 295 (1973).
[20]R. C. Vehse and E. T. Arakawa, Phys. Rev. 180, 695 (1969).
[21]A. C. Blodgett, Jr. and W. E. Spicer, Phys. Rev. 158, 514 (1967).
[22]F. Wooten, *Optical Properties of Solids* (Academic, New York, 1972).
[23]J. H. Weaver, Phys. Rev. B 11, 1416 (1975).
[24]J. H. Weaver, D. W. Lynch, and C. G. Olson, Phys. Rev. B 7, 4311 (1973).
[25]J. H. Weaver, D. W. Lynch, and C. G. Olson, Phys. Rev. B 10, 501 (1974).
[26]D. W. Lynch, C. G. Olson, and J. H. Weaver, Phys. Rev. B 11, 3617 (1975).
[27]W. Scott and L. Muldawer, Phys. Rev. B 9, 1115 (1974).
[28]S. Hüfner, G. K. Wertheim, and J. H. Wernick, Phys. Rev. B 8, 4511 (1973).
[29]W. Gudat and C. Kunz, Phys. Status Solidi B 52, 433 (1972).
[30]C. S. Wang and J. Callaway, Phys. Rev. B 9, 4897 (1974).
[31]M. Singh, C. S. Wang, and J. Callaway, Phys. Rev. B 11, 287 (1975).
[32]K. Kameswara Rao, T. J. Moravec, J. C. Rife, and R. N. Dexter, Phys. Rev. B 12, 5937 (1975).
[33]Kameswara K. Rao, Ph.D. thesis (University of Wisconsin, 1975) (unpublished).
[34]T. J. Moravec, Ph.D. thesis (University of Wisconsin, 1975) (unpublished).
[35]L. Holland, *Vacuum Deposition of Thin Films* (Chapman and Hall, London, 1970).
[36]S. Mader, in *Handbook of Thin Film Technology*, edited by L. I. Maissel and R. Glang (McGraw-Hill, New York, 1970), Chap. 9.
[37]I. H. Khan, in Ref. 36, Chap. 10.
[38]C. A. Neugebauer, in Ref. 36, Chap. 8.
[39]Von Hans-Martin Wiedenmann and H. Hoffman, Z. Angew. Phys. 18, 502 (1965).
[40]B. W. Veal and A. P. Paulikas, Phys. Rev. B 10, 1280 (1974).
[41]M. Altarelli and D. Y. Smith, Phys. Rev. B 9, 1290 (1974).
[42]Y. Onodera and Y. Toyozawa, J. Phys. Soc. Jpn. 24, 341 (1968).
[43]A. G. Thompson, Manuel Cardona, Kerry L. Shaklee, and J. C. Woolley, Phys. Rev. 146, 601 (1966).
[44]C. P. Wang (private communication).
[45]C. D. Gelatt, Jr. and H. Ehrenreich, Phys. Rev. B 10, 398 (1974).
[46]J. L. Robins and J. B. Swan, Proc. Phys. Soc. Lond. 76, 857 (1960).
[47]D. L. Misell and A. J. Atkins, Philos. Mag. 27, 95 (1973).
[48]C. Wehenkel and B. Gauthé, Phys. Status Solidi B 64, 515 (1974).